第 32 卷第 10 期
2016 年 10 月

无 机 化 学 学 报
CHINESE JOURNAL OF INORGANIC CHEMISTRY

Vol.32 No.10
1876-1884

基于半刚性的 4-羧基苯乙酸和富氮共配体组装的 Zn(Ⅱ)/Cd(Ⅱ)配位聚合物的合成、结构和性质

鞠丰阳[1] 李云平[2] 李桂连[2] 刘广臻*,[2] 辛凌云[2] 李晓玲[2]

([1]洛阳师范学院食品与药品学院,洛阳 471934)

([2]洛阳师范学院化学化工学院,洛阳 471934)

摘要:采用溶剂热法合成了一系列 Zn(Ⅱ)/Cd(Ⅱ)配位聚合物:$\{[Zn(cbaa)(bpmp)_{0.5}(H_2O)]\cdot 2H_2O\}_n$ (**1**)、$[Zn(cbaa)(bip)]_n$ (**2**)、$[Cd(cbaa)(Hizb)]_n$ (**3**)和$[Cd_2(cbaa)_2(itmb)(H_2O)]_n$ (**4**)(H_2cbaa=4-羧基苯乙酸;bpmp=1,4-二(4-吡啶甲基)哌嗪;bip=3,5-双(1-咪唑基)吡啶;Hizb=2-(4-咪唑-1-基苯基)-1*H*-苯并咪唑;itmb=1-(咪唑-1-基)-4-(1,2,4-三唑-1-基甲基)苯)。X 射线单晶衍射结果表明,半刚性的 4-羧基苯乙酸和富氮辅助配体构筑形成了 4 个多样化拓扑结构的配位聚合物。化合物 **1** 和 **2** 是 Zn(Ⅱ)配位聚合物:**1** 是由 2 个 Zn-羧酸盐链之间通过富氮配体桥连形成的一维梯形结构,而 **2** 是由 Zn-羧酸盐链之间通过富氮配体拓展形成的二维单层结构;化合物 **3** 和 **4** 是 Cd(Ⅱ)配位聚合物:**3** 是由 Cd-O 无机链之间通过羧酸配体的桥连拓展形成的二维单层结构,富氮配体作为伸出层平面的悬臂仅仅起到结构修饰作用,而 **4** 则形成了 Cd-羧酸盐空旷双层结构,富氮配体填充在层内空腔中,从而导致了致密双层结构的产生。另外,考察了 4 个化合物的热稳定性和光致发光性能。

关键词:溶剂热合成;锌;镉;配位聚合物;荧光

中图分类号:O0614.24+1;O614.24+2 **文献标识码**:A **文章编号**:1001-4861(2016)10-1876-09

DOI:10.11862/CJIC.2016.234

Zinc(Ⅱ) and Cadmium(Ⅱ) Coordination Polymers with Various Polynuclears Spaced by Semirigid 4-Carboxybenzeneacetate and Nitrogen-Rich Co-ligands: Syntheses, Structures and Properties

JU Feng-Yang[1] LI Yun-Ping[2] LI Gui-Lian[2] LIU Guang-Zhen*,[2] XIN Ling-Yun[2] LI Xiao-Ling[2]

([1]*School of Food and Drug, Luoyang Normal University, Luoyang, Henan* 471934, *China*)

([2]*College of Chemistry and Chemical Engineering, Luoyang Normal University, Luoyang, Henan* 471934, China)

Abstract: A series of four Zn(Ⅱ)/Cd(Ⅱ)) coordination polymers, $\{[Zn(cbaa)(bpmp)_{0.5}(H_2O)]\cdot 2H_2O\}_n$ (**1**), $[Zn(cbaa)(bip)]_n$ (**2**), $[Cd(cbaa)(Hizb)]_n$ (**3**) and $[Cd_2(cbaa)_2(itmb)(H_2O)]_n$ (**4**) have been obtained by the solvothermal reaction of Zn(Ⅱ)/Cd(Ⅱ) acetate with semirigid 4-carboxybenzeneacetic acid (H_2cbaa) and co-ligands, 1,4-bis(4-pyridyl-methy)piperazine (bpmp), 3,5-bis(1-imidazoly)pyridine (bip), 2-(4-imidazol-l-yl-phenyl)-1*H*-benzimidazole (Hizb) and 1-(imidazo-1-ly)-4-(1,2,4-trazol-1-ylmethyl)benzene (itmb). The single-crystal X-ray diffraction analyses show that four compounds feature various polynuclears spaced by 4-carboxybenzeneacetate and N-rich co-ligands and display various topology structures. Two zinc complexes are 1D ladder featuring Zn-carboxylate chains linked further by bpmp co-ligands for **1** and 2D monolayer containing Zn-carboxylate chains cross-linked further by bip co-ligands for **2**, respectively. And two cadmium complexes exhibit 2D monolayer featuring Cd-O inorganic chains cross-linked further by cbaa carboxylates with Hizb co-ligands acting as pendent arms for **3** and 2D dense bilayer

收稿日期:2016-06-30。收修改稿日期:2016-09-14。

国家自然科学基金(No.21571093)、河南省高校科技创新人才项目(No.14HASTIT017)、河南省高校科技创新团队项目(No.14IRTSTHN008)和河南省科技攻关计划(No.162102210304)资助。

*通信联系人。E-mail:gzliuly@126.com

containing Cd-carboxylate open bilayer with itmb co-ligands encapsulated within the cavities for **4**, respectively. The fluorescent properties and thermal stabilities of all these compounds have been investigated. CCDC: 906895, **1**; 1443786, **2**; 906897, **3**; 906898, **4**.

Keywords: 4-carboxybenzeneacetic acid; zinc; cadmium; coordination polymers; fluorescent properties

Carboxylate ligands are desirable candidates for the assembly processes of metal-organic coordination polymers (MOCPs) due to their excellent coordination capability and versatile binding modes under different reaction conditions[1-3]. Additionally, the deprotonation of carboxyl groups can compensate for the metal charge, which is necessary to avoid inclusion of unligated anionic species[4-5]. As is well known, the carboxylate groups are able to adopt numerous binding modes such as monodentate, bidentate, tridentate and tetradentate coordination[6-7]. The bidentate coordination modes are the most common ones and can be detailed as chelating, bridging syn-anti in μ_2-1,1 mode, *syn-syn*, *syn-anti*, and *anti-anti* in μ_2-1,3 mode[8-11]. And the tridentate modes can be illustrated as *anti-syn-syn*, *anti-syn-anti* in μ_3-1,1,3 mode, and so on[12-13]. To satisfy the coordination requirement, the tetradentate coordination mode called as *syn-anti-syn-anti* in μ_4-1,1,3,3 mode and the pentadentate coordination mode may be employed[14]. The rigid aromatic carboxylate ligands have been investigated universally due to the fact that their inherent large molecule stiffness can afford the MOCPs with high thermal stability[15-17]. And several researches based on flexible aromatic carboxylate ligands have been documented recently[18-21]. On the one hand, using flexible carboxylate ligands can result in "losing control" over the design and assembly of relevant MOCPs because flexible ligands are more sensitive to reaction conditions. Moreover, the rotation about the C-C bonds can lead to changeable conformation and low symmetry of carboxylate ligands. On the other hand, the flexibility of ligands may provide rare opportunities to construct some interesting crystalline architectures with particular attributes deriving from so-called breathing ability. Semirigid aromatic dicarboxylate ligands combined with rigid -COOH and flexible -CH_2COOH groups possess the merits of both rigid and flexible carboxylate groups, and have caught our attention successfully although they are underdeveloped in the chemistry of MOCPs[22-23].

Several complicated factors such as the nature of metal ions and carboxylate ligands, the concentration of starting species, solvent, temperature, pH value and N-donor co-ligands can influence the coordination modes of the carboxylate groups, in turn deciding the structures, properties and potential applications of resulted MOCPs[24-25]. Using N-donor co-ligands to meet or mediate the coordination modes of the carboxylate groups has been probed widely and always been an efficient approach for reconstructing the motifs of MOCPs[26-27]. Bis-pyridyl-type ligands are the most common ones among numerous N-donor co-ligands. And various nitrogen-rich co-ligands including a number of imidazolyl, triazolyl, tetrazolyl, pyrazolyl, benzimidazolyl and so on, which can provide more coordination sides and more chance to produce H-bonds interaction and aromatic interaction, have been involved and played important role in the assembly of MOCPs[28-30].

Herein, a series of four zinc and cadmium coordination polymers originating from Zn (Ⅱ)/Cd (Ⅱ) acetate, semirigid 4-carboxybenzeneacetic acid (H_2cbaa) and various nitrogen-rich co-ligands have been exemplified. Various coordination modes of $cbaa^{2-}$ observed in complexes **1~4** are shown in Scheme 1a~d.

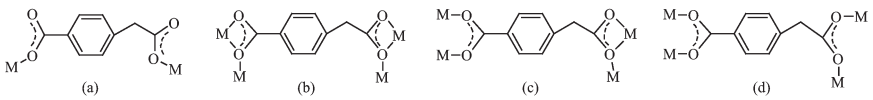

Scheme 1　Coordination modes of $cbaa^{2-}$ observed in complexes **1~4**

And the preparations, X-ray structures, fluorescent properties and thermal stabilities of all these compounds are described below.

1 Experimental

1.1 Materials and methods

All reagents were commercially purchased and used directly without further purification. Elemental analyses for C, H and N were performed on a Flash EA 2000 elemental analyzer. Infrared spectra (IR) were obtained by a Nicolet 6700 FT-IR spectrophotometer over a range of 4 000~600 cm^{-1}. The powder X-ray diffraction (PXRD) patterns of the products were recorded with a Bruker AXS D8 Advance diffractometer using monochromated Cu $K\alpha$ adiation (λ= 0.154 18 nm; generator current: 40 mA; generator voltage: 40 kV; scanning scope: 2θ=5°~50°). The thermogravimetric analyses (TGA) were carried out on a S Ⅱ EXStar6000 TG/DTA6300 analyzer with a heating rate of 10 ℃·min^{-1} under N_2 atmosphere. Luminescence spectra of the solid samples were obtained at the room temperature on a Hitachi F-4500 spectrophotometer with xenon arc lamp as the light source.

1.2 Preparation of complexes

The compounds were synthesized by the solvothermal methods using a mixed solvent of absolute methanol (3.50 mL), deionized water (3.50 mL) and NaOH (0.002 0 g, 0.05 mmol). Starting materials were placed in a sealed 23 mL PTFE-lined stainless steel autoclave and kept under autogenous pressure at 120 ℃ for 4 days, whereupon it was cooled slowly to the room temperature. The crystals were isolated after being washed with distilled water and acetone, and allowed to dry in air. The PXRD patterns of the bulk products are in well agreement with the simulated patterns based on the structure solutions (Fig.S1~S4).

Synthesis of $\{[Zn(cbaa)(bpmp)_{0.5}(H_2O)]\cdot 2H_2O\}_n$ (**1**): A mixture of $Zn(OAc)_2\cdot 2H_2O$ (0.044 g, 0.20 mmol), H_2cbaa (0.018 g, 0.10 mmol) and bpmp (0.027 g, 0.10 mmol) were dissolved in the mixed solvent, giving colourless blocked crystals afte solvothermal reaction (Yield: 83% based on Zn). Anal. Calcd. for $C_{17}H_{21}N_2O_7Zn$(%): C, 47.40; H, 4.91; N, 6.50. Found(%): C, 47.33; H, 4.56; N, 6.47. IR (KBr, cm^{-1}): 3 619(w, br), 2 933(w, br), 2 815(m), 1 618(s), 1 578(s), 1 525(s), 1 424(s), 1 350(s), 1 299(m), 1 158(m), 1 012(m), 929 (w), 841(m), 780(m), 727(m), 687(w), 615(w).

Synthesis of $[Zn(cbaa)(bip)]_n$ (**2**): A mixture of $Zn(OAc)_2\cdot 2H_2O$ (0.022 g, 0.10 mmol), H_2cbaa (0.009 0 g, 0.050 mmol) and bip (0.010 g, 0.050 mmol) were dissolved in the mixed solvent, giving colourless blocked crystals after solvothermal reaction (Yield: 41% based on Zn). Anal. Calcd. for $C_{20}H_{15}N_5O_4Zn$(%): C, 52.82; H, 3.32; N, 15.40. Found (%): C, 52.79; H, 3.34; N, 15.38. IR (KBr, cm^{-1}): 3 124 (m), 3 023(w), 2 893(w), 1 607(s), 1 561(s), 1 509(s), 1 359(s), 1 317 (m), 1 266(m), 1 120(m), 1 064(m), 1 007(m), 946(m), 882(m), 823(m), 732(m), 646(s).

Synthesis of $[Cd(cbaa)(Hizb)]_n$ (**3**): A mixture of $Cd(OAc)_2\cdot 2H_2O$ (0.053 g, 0.20 mmol), H_2cbaa (0.018 g, 0.10 mmol) and Hizb (0.026 g, 0.10 mmol) were dissolved in the mixed solvent, giving colourless blocked crystals after solvothermal reaction (Yield: 37% based on Cd). Anal. Calcd for $C_{25}H_{18}CdN_4O_4$ (%): C, 54.51; H, 3.29; N, 10.17. Found(%): C, 54.60; H, 3.22; N, 10.13. IR (KBr, cm^{-1}): 3 415(w, br), 3 191(w, br), 1 599(m), 1 563(m), 1 508(s), 1 391(s), 1 313(m), 1 277(w), 1 064(w), 843(w), 747(m), 679(w).

Synthesis of $[Cd_2(cbaa)_2(itmb)(H_2O)]_n$ (**4**): A mixture of Cd $(OAc)_2\cdot 2H_2O$ (0.053 g, 0.20 mmol), H_2cbaa (0.018 g, 0.10 mmol) and itmb (0.045 g, 0.20 mmol) were dissolved in the mixed solvent, giving colourless blocked crystals after solvothermal reaction (Yield: 64% based on Cd). Anal. Calcd for $C_{30}H_{25}Cd_2N_5O_9$(%): C, 43.71; H, 3.06; N, 8.50. Found (%): C, 43.67; H, 3.11; N, 8.48. IR (KBr, cm^{-1}): 3 292(w, br), 3 135(m), 1 607(s), 1 549(s), 1 523(s), 1 384(s), 1 276(m), 1 140 (m), 1 059(w), 1 018(w), 931(w), 835(w), 783(m), 739 (s), 659(s).

1.3 X-ray crystallography

Single-crystal X-ray diffraction data for complexes **1**~**4** were recorded at room temperature on a Bruker SMART APEX Ⅱ CCD diffractometer equipped with graphite-monochromated Mo $K\alpha$ radiation (λ= 0.071 073 nm). All the structures were solved by the

direct method followed by successive difference Fourier syntheses and refined by full-matrix least-squares techniques using the SHELX-97 program package with anisotropic thermal parameters for all non-hydrogen atoms[31-32]. Hydrogen atoms of the organic molecules were placed in calculated positions and refined isotropically with a riding model. The hydrogen atoms associated with the H_2O molecule were initially located in a difference Fourier map and included in the final refinement by use of geometrical restraints with the O-H distances being fixed at 0.085 nm and U_{iso}(H) equivalent to 1.5 times of U_{eq}(O). The details of the structure solution and final refinements are listed in Table 1.

CCDC: 906895, **1**; 1443786, **2**; 906897, **3**; 906898, **4**.

Table 1　Crystal and structure refinement data for 1~4

	1	2	3	4
Empirical formula	$C_{17}H_{21}N_2O_7Zn$	$C_{20}H_{15}N_5O_4Zn$	$C_{25}H_{18}CdN_4O_4$	$C_{30}H_{25}Cd_2N_5O_9$
Formula weight	430.73	454.74	550.83	824.35
Crystal system	Monoclinic	Monoclinic	Orthorhombic	Monoclinic
Space group	$P2_1/c$	$P2_1/n$	$P2_12_12_1$	$P2_1/c$
a / nm	1.081 92(3)	1.116 10(10)	0.790 77(10)	1.564 82(3)
b / nm	1.039 34(3)	1.468 70(12)	1.025 21(13)	0.939 46(2)
c / nm	1.695 94(6)	1.162 25(10)	2.646 2(3)	1.997 03(4)
β / (°)	103.286(3)	96.784(2)	90	96.198 0(19)
V / nm^3	1.856 0(10)	1.891 8(3)	2.145 3(5)	2.918 64(11)
Z	4	4	4	4
D_c / (g·cm^{-3})	1.541	1.597	1.705	1.876
μ / mm^{-1}	1.365	1.338	1.060	1.523
F(000)	892	928	1 104	1 632
θ range / (°)	3.15~25.49	2.24~25.49	2.51~25.50	2.99~25.50
Reflections collected, unique	7 148, 3 441	12 099, 3 510	6 762, 3 720	11 489, 5 421
R_{int}	0.024 0	0.024 3	0.027 6	0.023 3
Completeness to θ / %	99.8	99.8	98.0	99.8
Data, restraints, parameters	3 441, 0, 244	3 510, 0, 271	3 720, 0, 307	5 421, 0, 415
Goodness-of-fit	1.031	1.027	1.019	1.021
R_1	0.039 2	0.026 7	0.031 3	0.028 0
wR_2 [$I>2\sigma(I)$]	0.096 9	0.061 5	0.050 5	0.066 5
R_1 (all data)	0.051 0	0.033 5	0.044 4	0.033 4
wR_2 (all data)	0.104 6	0.064 3	0.055 0	0.070 3
Absolute structure parameter	—	—	0.04(3)	—
$(\Delta\rho)_{max}$, $(\Delta\rho)_{min}$ / (e·nm^{-3})	649, −487	266, −238	539, −392	676, −687

2　Results and discussion

2.1　Structural description of {[Zn(cbaa)(bpmp)$_{0.5}$(H$_2$O)]·2H$_2$O}$_n$ (1)

The asymmetric unit of complex **1** comprises one crystallographically distinct Zn(Ⅱ) cation, one cbaa^{2-}, half bpmp molecule, one coordinating H_2O molecule and two free H_2O molecules (Fig.1a). The Zn1 atom forms a slightly distorted tetrahedron [$ZnNO_2(H_2O)$] by one -COO$^-$ oxygen atom and one -CH$_2$COO$^-$ oxygen atom from two symmetry-related cbaa^{2-}, one pyridyl nitrogen atom of bpmp ligand and one O atom of coordinated water. The Zn-O bond lengths range from 0.196 4(2) to 0.204 7(2) nm, and the Zn-N bond length is 0.204 1(2) nm. The isolated [$ZnNO_2(H_2O)$] tetrahedras are spaced by cbaa^{2-} ligand to produce Zn-carboxylate chains, and the neighbor chains are linked by bpmp co-ligands to generate a ladderlike

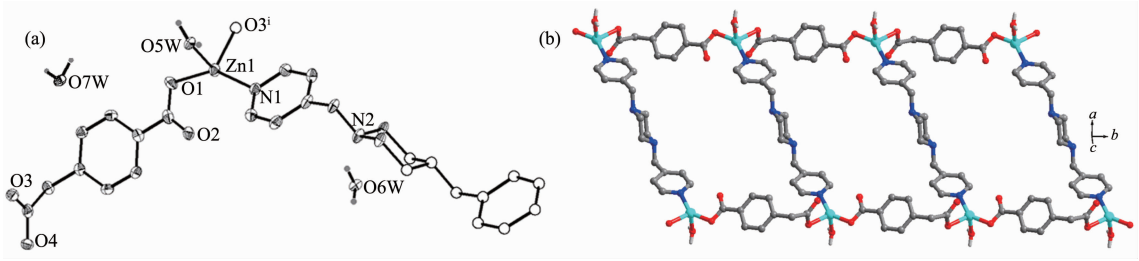

Displacement ellipsoids are drawn at the 30% probability level and all hydrogen atoms of carbon atoms are omitted for clarity; Symmetry codes: [i] x, y+1, z

Fig.1 (a) View of coordination environment of Zn(Ⅱ) in **1**; (b) Ladderlike coordination polymer along the b direction

coordination polymer propagating along the b direction (Fig.1b). Each stile of the ladder is comprised of $[ZnNO_2(H_2O)]$ tetrahedra connected by μ_2-cbaa^{2-} ligand with a bismonodentate mode for both carboxyalte groups. The μ_2-bpmp ligand acts as the rung of the ladder joining to Zn(Ⅱ) centers of the stiles through terminal pyridyl nitrogen atoms.

The parall ladders are closed packing such that each ladder is surrounded by six neighbours and cohered together by H-bonding interactions between the coordinated water and lattice water, leading to no solvent-accessible volume for the supramolecular structure (Fig.S5).

2.2 Structural description of [Zn(cbaa)(bip)]$_n$ (2)

The asymmetric unit of complex **2** consists of one Zn(Ⅱ) cation, one cbaa^{2-} and one bip molecule, as shown in Fig.2a. The unique Zn atom forms a slightly distorted tetrahedron $[ZnN_2O_2]$ by one -COO$^-$ oxygen atom and one -CH_2COO^- oxygen atom from two symmetry-related cbaa^{2-}, and two N atoms from two symmetry-related bip ligands. The Cd-O distances are 0.194 03(16) and 0.195 57(16) nm while the Cd-N distances are 0.201 18(16) and 0.203 78(16) nm. The $[ZnN_2O_2]$ units are connected by μ_2-cbaa^{2-} ligands with both carboxylate groups in monodentate mode to form a metal-carboxylate chain along the a direction and futher linked by the bip molecules along the c diretion to generate a square (4,4) grid monolayer (Fig.2b). The neighboring layers are cohered to produce a layer-pair by strong π-π stacking interactions derived from the pyridine rings of bip molecules with the centroid-centroid distances of 0.407 10(2) nm. And the layer-pairs are further stacked to form the ultimate 3D framework by relatively weak van der Waals interactions (Fig.S6).

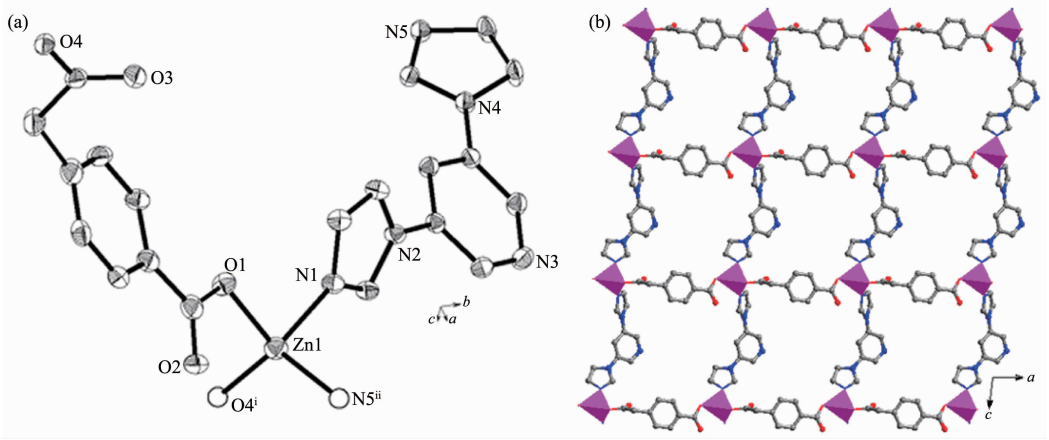

Displacement ellipsoids are drawn at the 30% probability level and all hydrogen atoms of carbon atoms are omitted for clarity; Symmetry codes: [i] x+1, y, z; [ii] x, y, z+1

Fig.2 (a) Coordinated environment of Zn(Ⅱ) in **2**; (b) Monolayer structure featuring $[ZnN_2O_2]$ units spaced by carboxylate and bip molecules

2.3 Structural description of [Cd(cbaa)(Hizb)]$_n$ (3)

The asymmetric unit of complex **3** consists of one Cd(Ⅱ) cation, one cbaa^{2-} and one Hizb molecule, as shown in Fig.3a. The unique Cd atom displays a [CdNO$_6$] heptacoordinated geometry with the coordination sphere defined by three -COO$^-$ oxygen atoms, three -CH$_2$COO$^-$ oxygen atoms and one imidazolyl N atom. The Cd-O distances range from 0.223 6(3) to 0.271 47(31) nm, and the Cd-N distance is 0.225 1(3) nm.

The Cd1 cations are doubly bridged with each other by two μ_2-O bridges from carboxylate groups to produce 1D motifs constructed by edge-shared [CdNO$_6$] polyhedra (Fig.3b). And the 1D motifs are interlinked by μ_2-cbaa^{2-} ligands to produce a monolayer structure in the ab plane with the Hizb ligands as pendent arms (Fig.3c and 3d), wherein both carboxylates of each cbaa^{2-} adopt a tridentate coordination mode. There are only intralayer H-bonds between benzimidazolyl N atoms and carboxylate O atoms, and the final 3D supramolecular structure is only stabilized by weak van der Waals forces between the layers.

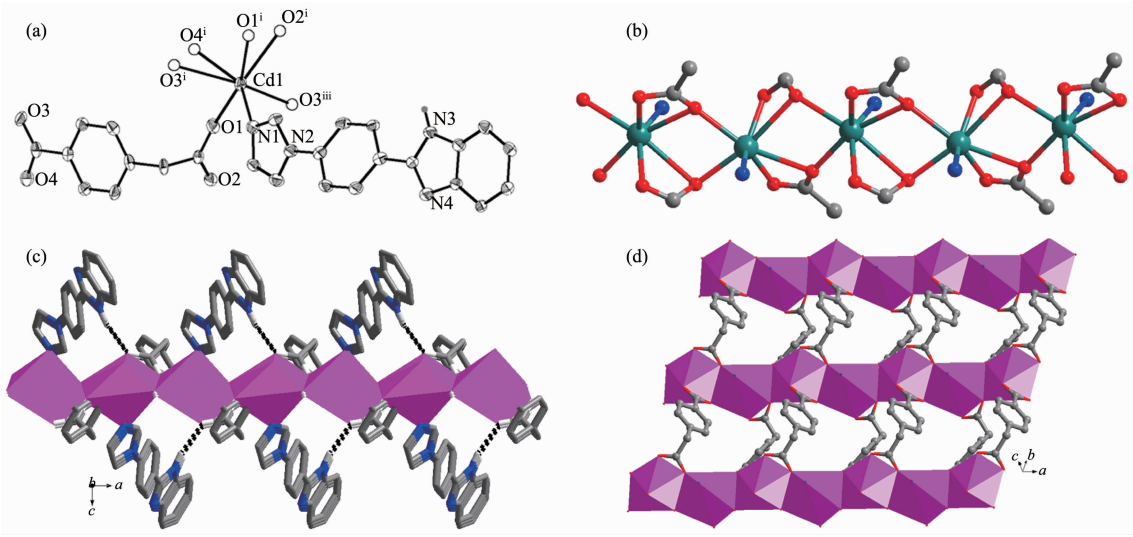

Displacement ellipsoids are drawn at the 30% probability level and all hydrogen atoms of carbon atoms are omitted for clarity; Symmetry codes: [i] $x-1/2, -y-1/2, -z$; [ii] $x-1/2, -y+1/2, -z$; [iii] $x, y+1, z$

Fig.3 (a) Coordinated environment of Cd(Ⅱ) in **3**; (b) Cd-carboxylate chain featuring edge-shared [CdNO$_6$] polyhedra; (c) Monolayer structure with Hizb pendent arms; the intralayer H-bonding interactions are labeled as dark dotted lines; (d) Cd-carboxylate sheet motif showing coordinated details of cbaa^{2-} ligand

2.4 Structural description of [Cd$_2$(cbaa)$_2$(itmb)(H$_2$O)]$_n$ (4)

The asymmetric unit of complex **4** consists of two Cd(Ⅱ) cations, two cbaa^{2-}, one itmb molecule and one guest water molecule, as shown in Fig.4a. Both Cd atoms display octahedrally coordinated geometries. The coordination sphere of Cd1 is formed by two -COO$^-$ oxygen atoms, two -CH$_2$COO$^-$ oxygen atoms, one water O atom and one terminal N atom of one itmb while the coordination sphere of Cd2 is defined by two -COO$^-$ oxygen atom, three -CH$_2$COO$^-$ oxygen atoms and one termial N atom of one itmb ligand. The Cd-O distances range from 0.221 9(2) to 0.251 5(2) nm, and the Cd-N distances are 0.232 8(3) and 0.234 7(3) nm, respectively.

Two Cd octahedra are triply bridged by the combination of one -CH$_2$COO$^-$ oxygen atom and two -COO$^-$ carboxylate groups in bridging bidentate mode to form one [Cd$_2$O(OCO)$_2$] dinuclear unit with the Cd…Cd seperation of 0.367 18(3) nm. The adjacent dinuclear units are further connected by one bridging bidentate-CH$_2$COO$^-$ carboxylate group to generate a single-stranded Cd-carboxylate chain along the *b* direction (Fig.4b). These Cd-carboxylate chains are

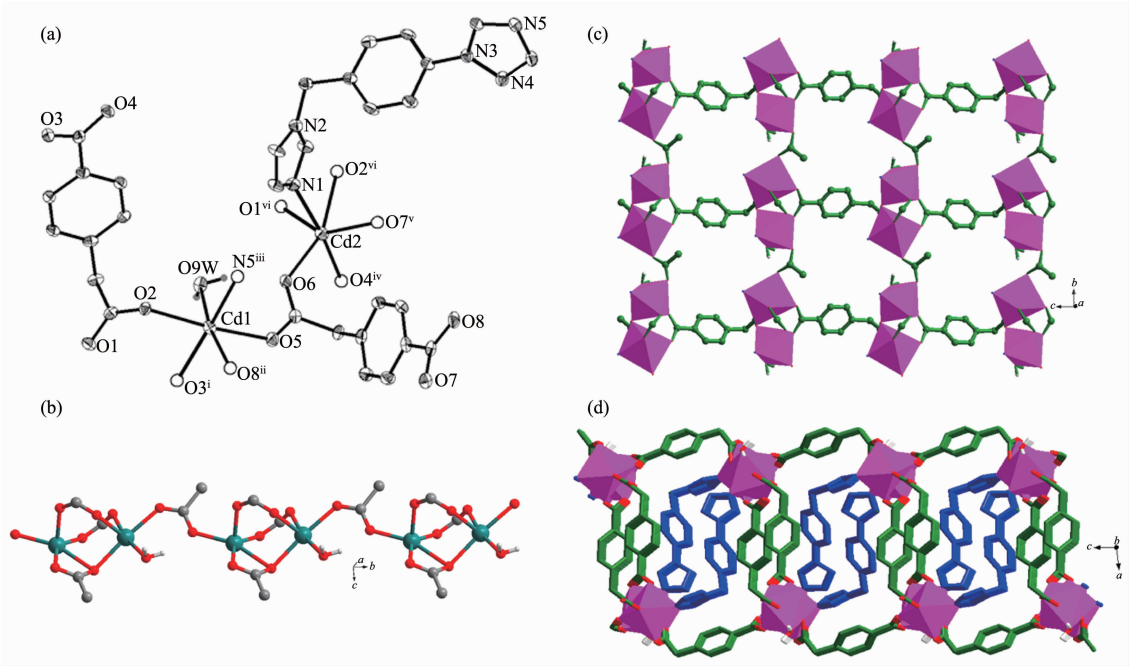

Displacement ellipsoids are drawn at the 30% probability level and all hydrogen atoms of carbon atoms are omitted for clarity; Symmetry codes: [i] $x, -y+1/2, z+1/2$; [ii] $-x, y-1/2, -z+1/2$; [iii] $-x, -y+2, -z$; [iv] $x, -y+3/2, z+1/2$; [v] $-x, y+1/2, -z+1/2$; [vi] $x, y+1, z$

Fig.4 (a) Coordinated environment of Cd(Ⅱ) in **4**; (b) Single-stranded chain featuring $\{Cd_2O(OCO)_2\}$ dinuclear unit spaced by bridging bidentate -CH_2COO^- carboxylate groups; (c) Cd-carboxylate sheet motif showing coordinated details of $cbaa^{2-}$ ligands; (d) Dense bilayer structure featuring open Cd-carboxylate bilayer with each channel filled with two stacking of itmb ligands acting simultaneously as the linkers between the chain motifs

extended by μ_2-$cbaa^{2-}$ ligands with two carboxylate groups in bridging bidentate and bridging tridentate coordination mode to produce one Cd-carboxylate sheet motif (Fig.4c). And the neighbor sheet motifs are connected through another μ_2-$cbaa^{2-}$ ligands with both carboxylate groups in bridging bidentate mode to generate one open Cd-carboxylate bilayer with linear channels paralleling to the chain motifs (Fig.S7). Furthermore, each channel is filled with two stacking of itmb ligands acting simultaneously as the linkers between the chain motifs, thus leading to final dense bilayer (Fig.4d). Meanwile, there are interlayer H-bonds between coordinated H_2O molecules and carboxylate O atoms to stabilize its entire 3D supramolecular structure (Fig.S8).

2.5 TGA and fluorescent properties

Thermogravimetric analysis (TGA) for complexes **1**~**4** were carried out on crystalline samples from room temperature to 900 ℃ to investigate their thermal stabilities, as shown in Fig.5. For complex **1**, the release of two guest water molecules was observed in the range from 61 to 182 ℃ with two obvious processes (Calcd. 8.36%, Found 7.84%). And the succeeding weight loss owing to the removal of one coordinated water and decomposition of organic ligands takes place between 280 and 860 ℃. The final residue holding a weight of 18.67% of the total sample is attributed to ZnO phase (Calcd. 18.89%). Complex **2** can survive below 310 ℃ and then a series of consecutive weight losses are observed and do not stop until the heating end. Similar to complex **2**, complex **3** can survive below 350 ℃ and then decomposes gradually until the heating end. The final residue is attributed to CdO component (Calcd. 23.31%, Found 24.02%). Complex **4** undergoes the first weight loss of 2.03 % in the temperature range of 110~155 ℃, which could be assigned to the release of one coordinated water molecule (Calcd. 2.18%). And the full decomposition of organic ligands appears at the temperature of 155~535 ℃. The remnant holding a

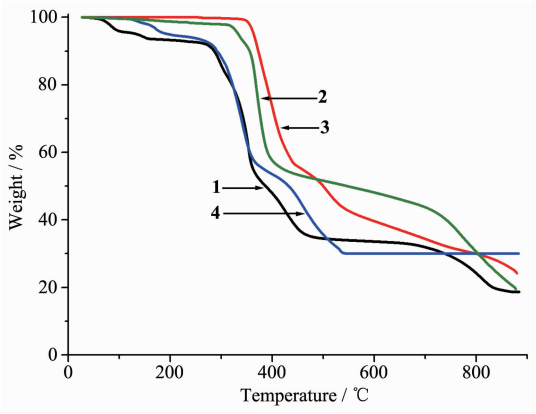

Fig.5　TGA curves of complexes **1**~**4**

weight of 30.17% of the total sample is CdO phase (Calcd. 31.15%).

The fluorescent properties of complexes **1**~**4** as well as the related ligands were investigated in the solid state at ambient temperature, as depicted in Fig. 6. The free H_2cbaa ligand has the emission with a maximum at 445 nm (λ_{ex}=353 nm). And the free nitrogen-rich co-ligands display featureless emissions with the maximum at 418 nm (λ_{ex}=290 nm) for bip, 466 nm (λ_{ex}=384 nm) for Hizb and 416 nm (λ_{ex}=350 nm) for itmp while the bpmp molecule shows weak fluorescent emission in the high-energy region and makes almost no contribution to the emission of the complex **1**[33]. Furthermore, there are multifarious emission behaviors with the maximum at 468 nm (λ_{ex}=300 nm) for **1**, 425 nm (λ_{ex}=349 nm) for **2**, 417 and 452nm (λ_{ex}=340 nm) for **3**, and 393 nm (λ_{ex}=300 nm) for **4**, respectively. They can probably be assigned to the ligand localized emission but neither metal-to-ligand charge transfer (MLCT) nor ligand-to-metal charge transfer (LMCT) in nature for the Zn^{2+} and Cd^{2+} with d^{10} configuration are difficult to oxidize or reduce [34-35]. Crystals of **1**, **2** and **4** show emission bands with spectrum features similar to that of the powdered H_2cbaa ligand. In comparison with the free H_2cbaa precursor, red shifts of emission bands for **1** and blue shifts of emission bands for **2** and **4** have been observed, which may be attributed to the deprotonated effect of H_2cbaa and the coordination interactions of the $cbaa^{2-}$ ligands around the central metal ions[36-37]. In addition, complex **3** displays fluorescence emission with bimodal bands which may be related to the cooperative actions of $cbaa^{2-}$ ligands and Hizb ligands.

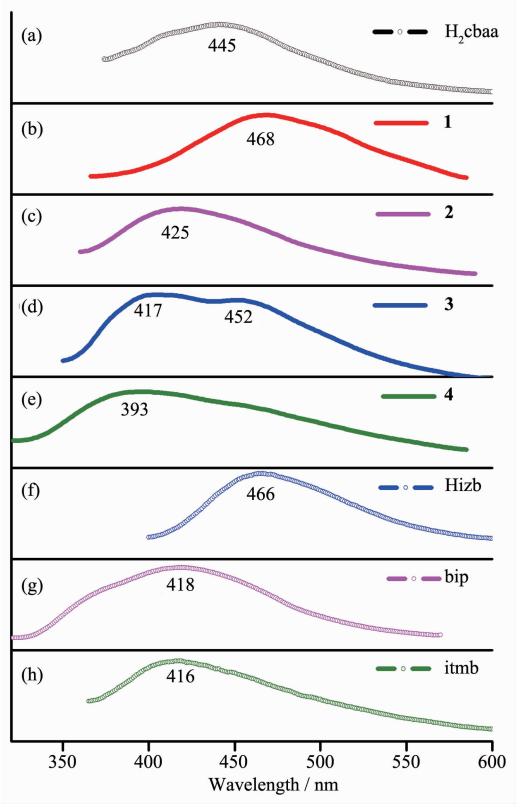

Fig.6　Solid-state emission spectra of complexes **1**~**4** and the related ligands at ambient temperature

3　Conclusions

In summary, the reactions of Zn(Ⅱ)/Cd(Ⅱ) acetate with semirigid 4-carboxybenzeneacetate and different nitrogen-rich co-ligands by mild solvothermal methods generate four new coordination polymers. Complex **1** and **2** possess 1D ladder and 2D monolayer structure featuring Zn-carboxylate chains linked by different nitrogen-rich co-ligands, respectively. Complex **3** exhibit 2D monolayer containing Cd-O inorganic chains cross-linked further by cbaa carboxylates with Hizb co-ligands acting as pendent arms, while complex **4** is 2D dense bilayer containing Cd-carboxylate open bilayer with linear channels filled with itmb co-ligands. Moreover, the solid state luminescences of all compounds are attributed to the ligand localized emission.

Supporting information is available at http://www.wjhxxb.cn

References:

[1] Yang L B, Wang H C, Fang X D, et al. *CrystEngComm*, **2016**,**18**:130-142

[2] Zeng M H, Wang Q X, Tan Y X, et al. *J. Am. Chem. Soc.*, **2010**,**132**:2561-2563

[3] Li G L, Liu G Z, Ma L F, et al. *Chem. Commun.*, **2014**,**50**:2615-2617

[4] Du M, Jiang X J, Zhao X J. *Inorg. Chem.*, **2007**,**46**:3984-3995

[5] Liu G Z, Li S H, Wang L Y. *CrystEngComm*, **2012**,**14**:880-889

[6] Ghosh A K, Shatruk M, Bertolasi V, et al. *Inorg. Chem.*, **2013**,**52**:13894-13903

[7] Zhang J P, Huang X C, Chen X M. *Chem. Soc. Rev.*, **2009**, **38**:2385-2396

[8] Lama P, Aijaz A, Neogi S, et al. *Cryst. Growth Des.*, **2010**, **10**:3410-3417

[9] Li X L, Liu G Z, Xin L Y, et al. *Synth. React. Inorg. Met.-Org. Chem.*, **2015**,**45**:914-920

[10]Li G L, Yin W D, Li X L, et al. *Synth. React. Inorg. Met.-Org. Chem.*, **2015**,**45**:869-874

[11]Ghosh S K, Ribas J, Bharadwaj P K. *Cryst. Growth Des.*, **2005**,**5**:623-629

[12]Su Z, Fan J, Chen M, et al. *Cryst. Growth Des.*, **2011**,**11**:1159-1169

[13]Dietzel P D C, Johnsen R E, Blom R, et al. *Chem. Eur. J.*, **2008**,**14**:2389-2397

[14]Xie F T, Bie H Y, Duan L M, et al. *J. Solid State Chem.*, **2005**,**178**:2858-2866

[15]Liu G Z, Li S H, Li X L, et al. *CrystEngComm*, **2013**,**15**:4571-4580

[16]Xin L Y, Li X L, Liu G Z. *Synth. React. Inorg. Met.-Org. Chem.*, **2013**,**43**:1013-1018

[17]YIN Wei-Dong(尹卫东), LI Gui-Lian(李桂连), LIU Guang-Zhen(刘广臻), et al. *Chinese J. Inorg. Chem.*(无机化学学报), **2015**,**31**(7):1439-1446

[18]Liu T F, Lü J, Cao R. *CrystEngComm*, **2010**,**12**:660-670

[19]Pigge F C. *CrystEngComm*, **2011**,**13**:1733-1748

[20]Zhou Y F, Wang R H, Wu B L, et al. *J. Mol. Struct.*, **2004**, **697**:73-79

[21]Xin L Y, Liu G Z, Ma L F, et al. *Aust. J. Chem.*, **2015**,**68**:758-765

[22]Liu G Z, Li X D, Li X L, et al. *CrystEngComm*, **2013**,**15**:2428-2437

[23]Tian Z F, Su Y, Lin J G, et al. *Polyhedron*, **2007**,***26***:2829-2836

[24]Long L S. *CrystEngComm*, **2010**,**12**:1354-1365

[25]Ma L F, Liu B, Wang L Y, et al. *Dalton Trans.*, **2010**,**39**:2301-2308

[26]Li C P, Chen J, Yu Q, et al. *Cryst. Growth Des.*, **2010**,**10**:1623-1632

[27]Jia W W, Luo J H, Zhu M L. *Cryst. Growth Des.*, **2011**,**11**:2386-2397

[28]Xue L P, Chang X H, Li S H, et al. *Dalton Trans.*, **2014**,**43**:7219-7226

[29]Xu J K, Sun X C, Yang L R, et al. *Z. Anorg. Allg. Chem.*, **2014**,**640**:236-242

[30]YIN Wei-Dong(尹卫东), LI Gui-Lian(李桂连), LI Xiao-Ling(李晓玲), et al. *Chinese J. Inorg. Chem.*(无机化学学报), **2016**,**32**(4):662-668

[31]Sheldrick G M. *SHELXS*-97, *Program for the Solution of Crystal Structures*, University of Göttingen, Germany, **1997**.

[32]Sheldrick G M. *SHELXL*-97, *Program for Refinement of Crystal Structures*, University of Göttingen, Germany, **1997**.

[33]Sahu J, Ahmad M, Bharadwaj P K. *Cryst. Growth Des.*, **2013**,**13**:2618-2627

[34]Zhang L P, Ma J F, Yang J, et al. *Inorg. Chem.*, **2010**,**49**:1535-1550

[35]QIAO Yu(乔宇), MA Bo-Nan(马博男), LI Xiu-Ying(李秀颖), et al. *Chinese J. Inorg. Chem.*(无机化学学报), **2015**,**31**(6):1245-1251

[36]Chang X H, Zhao Y, Feng X, et al. *Polyhedron*, **2014**,**83**:159-166

[37]Li F F, Ma J F, Song S Y, et al. *Inorg. Chem.*, **2005**,**44**:9374-9383